Earth Systems and Environment (2018) 2:305–322
https://doi.org/10.1007/s41748-018-0072-8

ORIGINAL ARTICLE

Particulate Matter Assessment Using In Situ Observations from 2009 to 2014 over an Industrial Region of Eastern India

Priyanjali Gogikar[1] · Bhishma Tyagi[1] · Rashmi Rekha Padhan[2,3] · M. Mahaling[2,4]

Received: 22 May 2018 / Accepted: 5 September 2018 / Published online: 17 September 2018

Abstract

The present study discusses the ambient air quality of an East Indian industrial region. The 8 hourly average concentrations of suspended particulate matter (SPM) and respirable suspended particulate matter (RSPM) for the period January 2009–December 2014 was analyzed at two industrial sites: Rourkela Township and Rajgangpur; and a residential site in the vicinity of industrial sites, i.e., Sonaparbat situated in Sundergarh District of Orissa State, India. The study area holds one of the biggest steel plants in India, cement factory and many medium- and small-scale industries in its surrounding area. To understand the contribution of the fine mode ($PM_{2.5}$—also called RSPM) and inhalable coarse particles (PM_{10}**—**also called SPM) to the particulate matter pollution, the ratio of $PM_{2.5}/PM_{10}$ is considered over the industrial and residential sites. Sonaparbat is loaded with more PM_{10} (particles concentration > 250 μg/m^3) and dominance of $PM_{2.5}$ was noticed during the years 2013 and 2014 compared to Rourkela and Rajgangpur. To detect the presence of specific emission sources that enhance the pollution over receptor sites, the conditional probability function and conditional bivariate probability function techniques are employed in the present study. Concentration weighted trajectory analysis using the 2-day back trajectory (by HYSPLIT-4 model) is also employed in the present study to discover the impact of transboundary pollution. Calm and weak wind speeds (< 1.5 ms^{-1}) are noticed over the study area, thereby indicating the pollution due to local sources present in and around the city. Rourkela Steel Plant, Orissa Cements Limited (OCL), OCL Iron and Steel along with vehicular exhaust are some of the major local sources situated within the vicinity of 5 km in the study area. The results show that pollution levels have a significant contribution from adjacent industrial areas apart from local emission sources, especially in the northwesterly and southeasterly directions. Further, an attempt has been made to investigate the dispersion of pollutants from the study site to the nearby regions during the study period by employing the 48-h seasonal forward trajectory analysis using the HYSPLIT-4 model.

Keywords Particulate matter · Source apportionment · Conditional bivariate probability function · Concentration weighted trajectory analysis · HYSPLIT 4

1 Introduction

Particulate matter (PM) is responsible for environmental issues like acid rain, impairment of vision, alteration of atmospheric radiation budget and modification of cloud properties (U.S. EPA 2004). The rapid growth of urbanization and industrialization is a significant factor for enhanced pollution levels of aerosols in developing countries like India (Karar et al. 2006; Karagulian et al. 2015). PM is a critical component of air pollution, and it has been found that elderly living in underdeveloped and developing countries have been experiencing a loss of healthy life-years (Health Effects Institute 2018).

✉ Bhishma Tyagi
bhishmatyagi@gmail.com

[1] Department of Earth and Atmospheric Sciences, National Institute of Technology Rourkela, Rourkela, Odisha 769008, India

[2] State Pollution Control Board, Odisha, Regional Office, Rourkela, Rourkela, Odisha 769002, India

[3] Present Address: State Pollution Control Board, Odisha, Regional Office, Angul, Angul, Odisha 759128, India

[4] Present Address: State Pollution Control Board, Odisha, Regional Office, Paradeep, Paradeep, Odisha 754142, India

PM is characterized by fine mode and coarse mode particles depending on their aerodynamic diameter of less than or equal to 10–2.5 µm (Nel 2005). Natural processes such as dust storms and re-suspension of soil dust are some of the major contributors for coarse mode particles, whereas anthropogenic sources such as vehicular emissions and industrial activities are the major contributors for fine mode particles (Querol et al. 2004). $PM_{2.5}$ mainly includes primary and secondary products resulting from combustion (Li et al. 2004). $PM_{2.5}$ is more hazardous compared to PM_{10}, because of its small size, longer lifetime and associated severe health effects (Dominici et al. 2014).

The PM concentrations are enhanced not only because of local emissions, but also by the transportation of pollutants from different regions (Cheng et al. 2013; Gogikar and Tyagi 2016). Meteorology in any region affects the state of pollution as they govern advection and dispersion (Jayamurugan et al. 2013). Thus to reduce the contamination of air due to various pollutants, policy makers need to recognize pollutants concentration, meteorological conditions and source areas, which are responsible for elevating the concentrations (Begum et al. 2005; Briggs and Long 2016). To investigate the regional transport of PM, source apportionment emerges as a powerful tool (e.g., Kotchenruther 2016; Liu et al. 2016; Cheng et al. 2016; Masiol et al. 2017). Source apportionment can be useful to know the impact of local pollution in any industrialized area or to quantify the effect of transported pollutants in the case of nearby industrial or mining area to any site (e.g., Grigoras et al. 2012; Sarasamma and Narayanan 2014; Li et al. 2017).

In the present study, the state of pollution by $PM_{2.5}$ and PM_{10} over an industrial area of Eastern India has been investigated. Eastern Indian region is home to most of the mining areas, power plants, cement factories and metal industry plants (Garg et al. 2001). Hence, the pollution levels are crucial to understand and maintain the air quality over the region. Specifically, the study aims to explore:

1. Temporal variation of $PM_{2.5}$, PM_{10} and $PM_{2.5}/PM_{10}$ and meteorological parameters such as temperature and humidity using in situ observations at three monitoring stations in different parts of an industrialized township, situated in Sundergarh District of Odisha State during the study period 2009–2014.
2. Seasonal variation of $PM_{2.5}$, PM_{10}, $PM_{2.5}/PM_{10}$ and air quality index (AQI) along with the seasonal pollution roses to investigate the dependency of pollutants over wind speed and wind direction during different seasons.
3. The identification of local and regional-scale impacts using seasonal conditional probability function analysis (CPF), conditional bivariate probability function analysis (CBPF) and seasonal weighted concentration weighted trajectory (WCWT) functions to locate possible source regions that are responsible for the enhancement of $PM_{2.5}$ and PM_{10} concentrations over the study area.
4. Seasonal forward trajectory analysis to have an insight over the dispersion of pollutants by air masses originating over the study site to different sinking areas in the next 48 h.

2 Study Area

To analyze the impact of the industries present in the eastern part of India, three monitoring stations, viz. Sonaparbat (22.184864°N, 84.875034°E), Rourkela (22.2604°N, 84.8536°E) and Rajgangpur (22.1902°N, 84.5799°E) are considered for the present study (shown in Fig. 1). Sonaparbat is a residential area, whereas Rajgangpur is an industrialized area associated with various industries such as cement, iron and steel industries (e.g., Orissa Cement Limited (OCL), OCL Iron and Steel etc.) at a spatial distance of 40 km from Rourkela. Major industries situated in the immediate neighborhood of Rourkela (within a radius of 10 km) are shown in Fig. 1. Rourkela has a steel plant and other industries along with residential areas around the city. The spatial extent of Rourkela is 121.7 sq. km with a population of 689 298 (Census report 2011). Brahmani River, which is the second largest river of Odisha, and one of the 14 major river systems of the country formed by the merging of perennial Koel and Sankh Rivers, flows near the major industrial town of Rourkela. Rourkela is popularly known as steel city of India, and is associated with the largest steel plant known as Rourkela Steel Plant, maintained by the Steel Authority of India Limited (SAIL) with a production of 15.7 million tons of hot metal, 14.3 million tons of crude steel and 12.4 million tons of saleable steel per annum (SAIL, Annual Report 2015–2016). The area also has small hills named Durgapur hills (~ 100–150 m). Rourkela has a tropical climate most of the year and experiences heavy rains during the monsoon (Kavuri et al. 2013). The region has ~ 300 km spatial distance from the Bay of Bengal in the south to the southeast direction.

3 Data Description

Observations of PM_{10} and $PM_{2.5}$ have been collected at a temporal resolution of every 8 h in a day, along with observations of temperature and humidity at a temporal resolution of 6 h in a day for the period 2009–2014 at Sonaparbat and Rourkela, and 2013–2014 at Rajgangpur by the State Pollution Control Board (SPCB), Odisha. Gravimetric, tapered element oscillating microbalance (TEOM) and beta

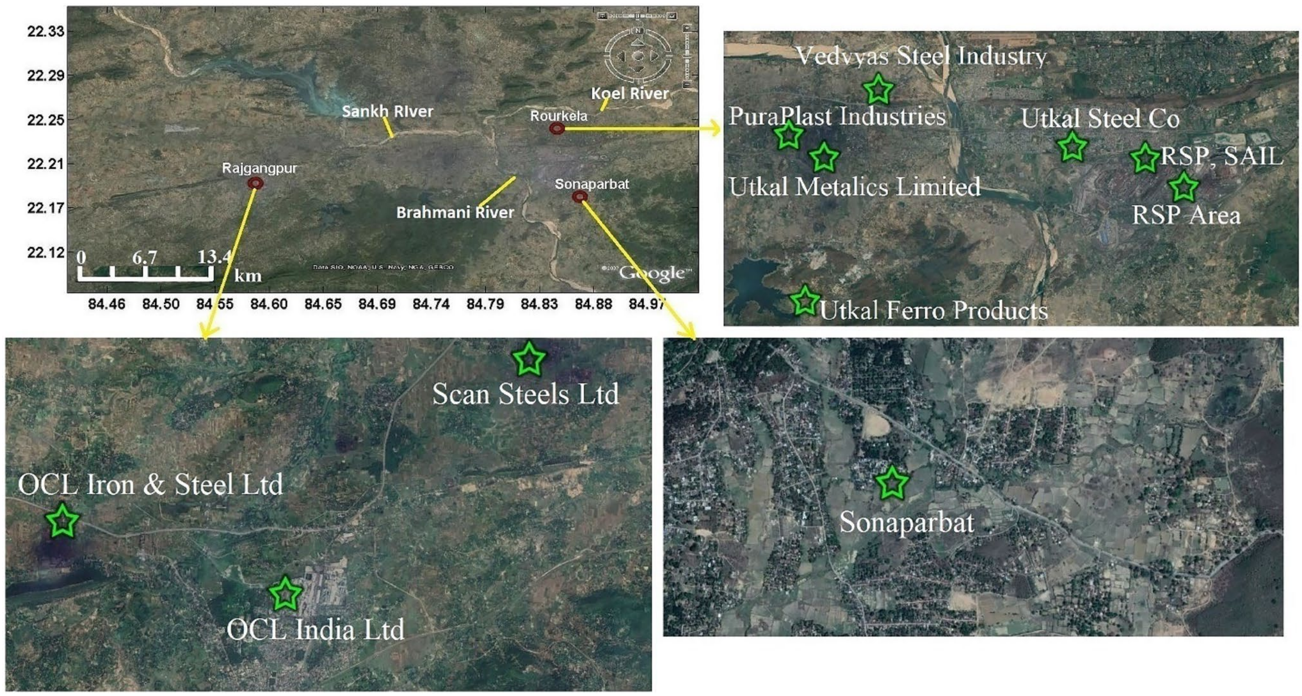

Fig. 1 Sitemap of Sundergarh showing the three monitoring stations Rajgangpur, Rourkela, Sonaparbat (shown as red circles in the sitemap) along with the major industries and residential areas marked as green stars located within the vicinity of monitoring stations

attenuation methods are adopted for PM monitoring by the Pollution Control Board (CPCB Report 2015). The year has been divided into four seasons in the present study as pre-monsoon (March to May), monsoon (June to September), post-monsoon (October to November) and winter (December to February). The surface wind speed and wind direction observations were absent at these monitoring stations. To get an insight into surface wind variations, we have used wind data (from 2010 to 2014) at a nearby station Kuarmunda (22.306611°N 84.779539°E), which is located at a spatial distance of 9 km from Rourkela, collected from Indian Space Research Organization (ISRO)—Meteorological and Oceanographic Satellite Data Archival Centre (MOSDAC) (http://mosdac.gov.in/data), which can be considered as one of the limitations in the present study. Seasonal pollution roses, seasonal CPF and seasonal CBPF are performed using the wind direction and wind speed data from MOSDAC. For performing the back trajectory analysis, NCEP/NCAR (National Centers for Environmental Prediction/National Center for Atmospheric Research) GDAS (Global Data Assimilation System) 1° data and HYSPLIT model (Draxler 1999; Draxler and Hess 1997, 1998; Stein et al. 2015) were used in the present study. Su et al. (2015) have found that GDAS 1° is better in the computation of back trajectories in comparison to GDAS 0.5° data as it is not incorporated with vertical velocity. Hence in the present study, GDAS 1° data is used for computation of back trajectories.

4 Methodology

The diurnal and seasonal variations of PM over the study area were analyzed for the period of study. Meteorological parameters, e.g., temperature and humidity, were considered to investigate the meteorological conditions associated with variation of $PM_{2.5}$ and PM_{10}at the industrial and residential monitoring stations. Further, attention was given to source apportionment to identify possible local and transboundary pollution sources using CPF, CBPF and CWT techniques. The methodology adopted for these source apportionment techniques are explained in following sections.

4.1 Conditional Probability Function (CPF) and Conditional Bivariate Probability Function (CBPF)

The probability that a particular source of emission lies in the considered wind sector is calculated by the conditional probability function (CPF) (Uria-Tellaetxe and Carslaw 2014) and is mathematically given in Eq. (1) as follows:

$$\mathrm{CPF} = \frac{A_{\Delta w}/C \geq T}{B_{\Delta w}} \quad (1)$$

where Δw indicates the wind sector, $A_{\Delta w}$ indicates the number of samples in the wind sector 'w' associated with concentration C exceeding the critical percentile concentration T and $B_{\Delta w}$ indicates the total number of samples in the wind sector 'w'. To calculate $A_{\Delta w}$, the highest 20% of source contribution concentrations are considered in the present study.

The CBPF analysis combines CPF to the bivariate polar plot where wind speed acts as a third variable and is extremely helpful in source characterization (Uria-Tellaetxe and Carslaw 2014; Rai et al. 2016). The CBPF generally deals with pollutant concentrations ($PM_{2.5}$ and PM_{10} concentration in the present study), wind speed (Δs) and direction (Δw). Mathematically, CBPF is given as follows (Eq. (2)):

$$\mathrm{CBPF} = \frac{A_{\Delta w,\Delta s}/C \geq T}{B_{\Delta w,\Delta s}} \tag{2}$$

The CBPF method considers the complete dispersion of the pollutant concentration instead of a value exceeding the specified critical value (Tiwari et al. 2017). The surface wind speed and wind direction along with the $PM_{2.5}$ and PM_{10} concentrations are considered to perform CPF and CBPF analysis using R-*openair* software package.

4.2 Back Trajectory Analysis

The CPF and CBPF methods explain the direction in which sources are situated and cannot estimate the location of the source areas (Pekney et al. 2006). The CWT method is efficient not only in identifying the location of the source areas, but also gives an insight over transboundary pollution (Dimitriou 2015a, b). To perform CWT, 2 days (− 48 h) backward trajectories at an elevation of 500 m above the ground level at an interval of 6 h (i.e., 00, 06, 12 and 18 UTC of every day) were computed using 1°GDAS data with HYSPLIT 4 model (Draxler and Hess 1998). These back trajectories are further used to analyze the aerosol transport pathways at Rourkela in conjunction with the observational data of $PM_{2.5}$ and PM_{10} for the computations of CWT. Two days forward trajectories were also included in the study to observe the pollutants' dispersion that originated from the study site to different receptor sites.

4.3 Concentration Weighted Trajectory (CWT)

CWT aims at producing an overview of the source regions that are responsible for the enhancement of PM levels over a particular area. CWT for $PM_{2.5}$ and PM_{10} over a specific grid cell (i, j) will determine the potential of the source at the study region and is mathematically given as (Eq. (3) and Eq. (4)) (Dimitriou 2015a, b):

$$P_{ij} = \frac{\sum_{x=1}^{n} P_x u_{ijx}}{\sum_{x=1}^{n} u_{ijx}} \tag{3}$$

$$M(i,j) = \begin{cases} 1.0\left(3\mathrm{V_{avg}} < \mathrm{V_{ij}}\right) \\ 0.7\left(1.5\mathrm{V_{avg}} < \mathrm{V_{ij}} < 3\mathrm{V_{avg}}\right) \\ 0.4\left(\mathrm{V_{avg}} < \mathrm{V_{ij}} < 1.5\mathrm{V_{avg}}\right) \\ 0.2\left(\mathrm{V_{ij}} < \mathrm{V_{avg}}\right) \end{cases} \tag{4}$$

P_{ij} in Eq. (3) indicates the concentration of PM in the (i, j) grid cell, P_x indicates the concentration of the X^{th} trajectory at the end point, n indicates the number of trajectory end points in the corresponding (i, j) grid and U_{ijx} indicates the total number of X_{th} trajectory end points in the corresponding (i, j) grid. Equation (4) indicates the weight function and determines the average number (V_{avg}) of pathways of the corresponding grid cells which are associated with at least one trajectory point and the number (V_{ij}) of pathway points in the grid cell (i, j) relationship. CWT analysis is used to examine the strengths of the source regions, and regional and transboundary PM distribution over the study site. The CWT method is employed in the present study as it is efficient in differentiating moderate sources from stronger or principal sources of pollution that are responsible for the enrichment of pollutants concentration over the study site (Hsu et al. 2003; Seibert et al. 1994).

5 Results and Discussion

5.1 Temporal Variation of Meteorological Parameters

The temporal variation of temperature and humidity from January 2009 to December 2014 for Sonaparbat and Rourkela stations and January 2013 to December 2014 for Rajgangpur station was analyzed. Sonaparbat, which is a residential area, experiences a maximum and minimum temperature of 45 °C and 9 °C in the pre-monsoon and winter, respectively. Maximum and minimum relative humidity was 90% in the post-monsoon and 26.5% in the winter season. At Rourkela, the maximum temperature was 44 °C, and the minimum temperature was 9 °C during the pre-monsoon and winter seasons, respectively. The relative humidity was high in winter, i.e., 92% and low in the pre-monsoon season, i.e., 11%. At Rajgangpur, the highest temperature was recorded in the pre-monsoon season with a value of 41.8 °C and the lowest temperature was recorded as 12 °C in winter. The relative humidity is high with a value of 95.3% during the post-monsoon season and low in winter season with a value of 17% during the study period. The average relative humidity was always greater than 60% at Sonaparbat and Rajgangpur stations and greater than 55% at Rourkela station during the study period. Sonaparbat shows higher values of humidity at lower ranges compared to the other two stations and the reason for this may be attributed to greater vegetation in the Sonaparbat area compared to Rourkela and Rajgangpur, where there are more industrial areas. The higher temperatures indicate high levels of the mixed layer over the region, and lower temperatures are responsible for a shallower mixed layer. The shallow mixed layer will cause a high concentration of pollutants compared to a higher mixed layer, and therefore the winter season is expected to have higher values of PM over the region, governed by local meteorological conditions.

The region experiences severe thunderstorms during the pre-monsoon season (Ray et al. 2014). The high relative humidity (> 80%) during the pre-monsoon season may correspond to the days with thunderstorms and lower humidity during non-thunderstorm days. During the post-monsoon season, there is a steep decrease in temperatures, whereas relative humidity remains high, which may be attributed to water/moisture, accumulated during monsoon season, and to western disturbances reaching over the region at times. Moreover, during 2013 and 2014 the catastrophic effect of severe cyclones, namely Phailin (08 October 2013 to 14 October 2013) and Hudhud (07 October 2014 to 14 October 2014), might have contributed to a high relative humidity during the post-monsoon season (Lakshmi et al. 2017). During winter, low temperatures were recorded at all the three monitoring stations, but relative humidity remained high (> 60%). Saraf et al. (2010) stated that the presence of local water bodies might contribute more moisture into the lower levels of the atmosphere and are responsible for high relative humidity in winter. As Brahmani River flows across the city, it might be responsible for more moisture in the atmosphere during the winter season, as there is more water accumulated in the river basin after the monsoon rainfall. The presence of high relative humidity in the atmosphere promotes the growth and production of secondary particles, thereby altering the size and optical properties (Wang and Martin 2007).

5.2 Temporal Variation of $PM_{2.5}$ and PM_{10}

The daily 8 h concentrations of $PM_{2.5}$, PM_{10} and ratio of $PM_{2.5}/PM_{10}$ are shown in Fig. 2 for the period January 2009–December 2014 for the Sonaparbat and Rourkela sites and from January 2013 to December 2014 for the Rajgangpur site. From Fig. 2a, b, it can be noticed that the concentrations of $PM_{2.5}$ and PM_{10} were always high during the study period for both industrial sites Rourkela and Rajgangpur as well as the residential site Sonaparbat. The thresholds of PM specified by CPCB, India, for daily values are 60 μg/m^3 ($PM_{2.5}$) and 100 μg/m^3 (PM_{10}), and 40 μg/m^3 ($PM_{2.5}$) and 60 μg/m^3 (PM_{10}) for annual values (CPCB report 2015). The dashed horizontal lines in Fig. 2a, b show the threshold values of daily $PM_{2.5}$ and PM_{10}. The annual mean concentrations of $PM_{2.5}$ and PM_{10} presented in Table 1 for all the

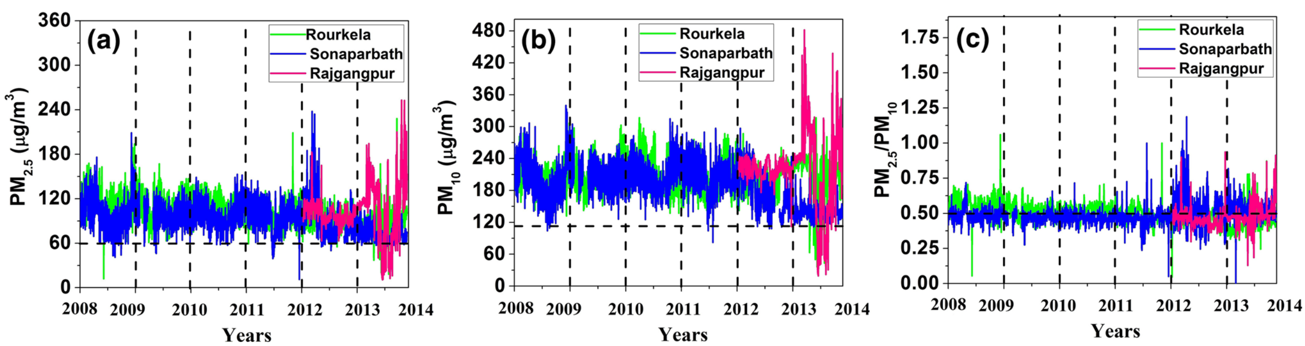

Fig. 2 Daily average variation of **a** $PM_{2.5}$, **b** PM_{10} and **c** $PM_{2.5}/PM_{10}$ for the three monitoring stations Rourkela, Sonaparbat and Rajgangpur stations. The dashed horizontal lines indicate the threshold values specified by CPCB and vertical dashed lines indicate years in the period of study. The year on the x-axis marks the end of particular year (i.e. 2008 means 31 December 2008)

Table 1 Annual mean mass concentrations of $PM_{2.5}$ and PM_{10} at Sonaparbat, Rourkela and Rajgangpur monitoring sites for the period of study

Year	Sonaparbat		Rourkela		Rajgangpur	
	$PM_{2.5}$ (μg/m^3)	PM_{10} (μg/m^3)	$PM_{2.5}$ (μg/m^3)	PM_{10} (μg/m^3)	$PM_{2.5}$ (μg/m^3)	PM_{10} (μg/m^3)
2009	102.15 ± 25.98	207.46 ± 44.70	114.69 ± 21.17	205.49 ± 27.36	–	–
2010	99.98 ± 18.70	211.30 ± 32.08	109.49 ± 19.63	210.65 ± 28.73	–	–
2011	99.10 ± 19.12	211.44 ± 34.32	108.63 ± 15.49	209.50 ± 32.64	–	–
2012	98.38 ± 21.30	212.35 ± 37.08	97.55 ± 16.46	200.21 ± 33.08	–	–
2013	95.25 ± 32.77	181.27 ± 40.30	92.82 ± 14.14	196.93 ± 27.64	99.84 ± 13.49	221.09 ± 14.66
2014	71.56 ± 11.13	141.99 ± 21.35	88.66 ± 21.01	203.45 ± 49.7	108.43 ± 49.93	221.11 ± 94.15

three monitoring stations indicate that concentrations always crossed the threshold limit throughout the study period.

The high concentrations of $PM_{2.5}$ and PM_{10} at the monitoring stations Rajgangpur and Rourkela may be due to local industrial emissions in the area. Higher values of $PM_{2.5}$ are also noticed at Sonaparbat, which is a residential area. These higher concentrations may be because of the geographic location of Sonaparbat in the proximity to an industrial region, i.e., Rourkela, from where transport of pollutants is very likely. The average daily variation of the $PM_{2.5}/PM_{10}$ ratio analysis indicates that the annual average values of the ratios are 0.5063 ± 0.7748, 0.5038 ± 0.1167 and 0.4760 ± 0.0821 at Sonaparbat, Rourkela and Rajgangpur stations, respectively. High values of ratio are attributed to particulate pollution caused by anthropogenic activities and lower values indicate pollution caused by natural sources (Sugimoto et al. 2016). From the $PM_{2.5}/PM_{10}$ ratios, it is clear that Sonaparbat, which is a residential site, is loaded with more $PM_{2.5}$ when compared to that of highly industrialized areas, Rourkela and Rajgangpur, and is experiencing a severe threat to the people residing there.

To have an understanding of the concentrations of $PM_{2.5}$ and PM_{10} that cross the threshold levels, percentage contributions of concentrations have been addressed in this study (shown as pie-charts). From the percentage contribution plot (Fig. 3), it is clear that for Rourkela (Fig. 3a), about 50.29% of $PM_{2.5}$ is in the concentration range of 50–100 μg/m^3 and 47.37% of $PM_{2.5}$ is in the concentration range of 100–150 μg/m^3. When PM_{10} is considered (Fig. 3d), particle concentration ranges between 200 and 250 μg/m^3, contributing to about 47.26%. For residential site Sonaparbat (Fig. 3b), 59.35% of the contribution is noticed for $PM_{2.5}$ ranging between 50 and 100 μg/m^3, which is found to be greater than the contribution made by similar particles at industrial sites Rourkela and Rajgangpur, and 37.94% of PM_{10} is observed to be in the range of 100–150 μg/m^3. Similarly, 35.22% of PM_{10} (Fig. 3e) is found to be observed in the range of 200–250 μg/m^3. For Rajgangpur station (Fig. 3c), 48.15% of $PM_{2.5}$ is categorized in the range of 100–150 μg/m^3 and 35.69% is contributed by the particles associated with the concentration of 50–100 μg/m^3, and 61.62% of PM_{10} (Fig. 3f) is contributed by the particles in the concentration range of 200–250 μg/m^3. When the PM_{10} particles with a concentration greater than 250 μg/m^3 are considered, Rourkela, Sonaparbat and Rajgangpur were found to be loaded by 7.92, 10.9 and 19.19%, respectively, during the study period. From the percentage contributions, it is very clear that Sonaparbat, which is a residential site, is loaded with more PM when concentrations of 50–100 μg/m^3 and > 250 μg/m^3 are considered when compared to the industrial site, Rourkela, which indicates an alarming pollution load and severe threat to the people residing over the site.

5.3 Seasonal Variation of $PM_{2.5}$, PM_{10} and $PM_{2.5}/PM_{10}$ Ratio

Wind speed and direction are primarily responsible for transporting and dispersion of contaminants from one region to the other (Guttikunda and Gurjar 2012). Seasonal variations of surface wind speed and direction along with $PM_{2.5}$ and PM_{10} were analyzed over the region (from 2010 to b2014) using pollution roses plots shown in Figs. 4 and 5. From the seasonal pollution rose plot for $PM_{2.5}$, during the pre-monsoon season (Fig. 4a), it is clear that the dominant wind direction is southeasterly and is associated with a concentration range of 80–100 μg/m^3 and fewer components were found in the easterly and northwesterly direction with a concentration range of 100–100.67 μg/m^3 and 80–100 μg/m^3, respectively. In the monsoon season (Fig. 4b), the dominant wind direction was southeasterly and it is majorly associated with the pollutants' concentration ranging from 80 to 100 μg/m^3 and fewer components were found in the northeasterly and easterly directions.

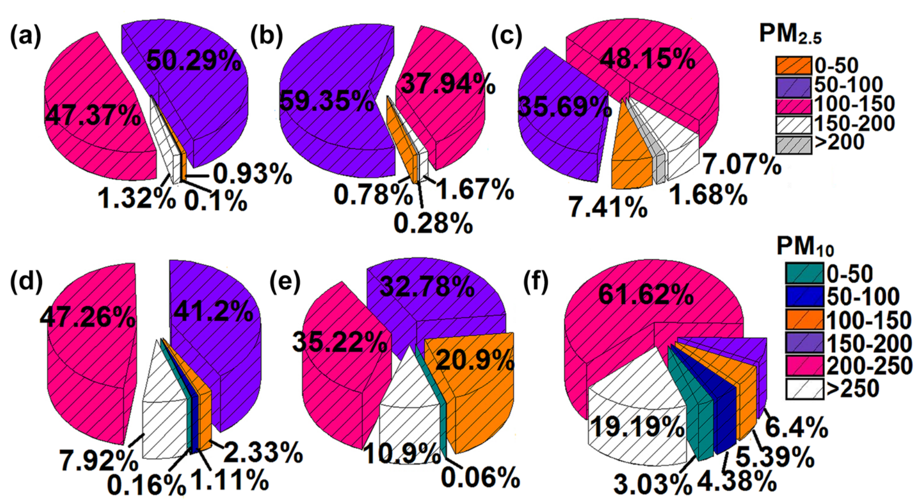

Fig. 3 Percentage contribution of $PM_{2.5}$ at **a** Rourkela, **b** Sonaparbat, **c** Rajgangpur, and for PM_{10} at **d** Rourkela, **e** Sonaparbat, **f** Rajgangpur

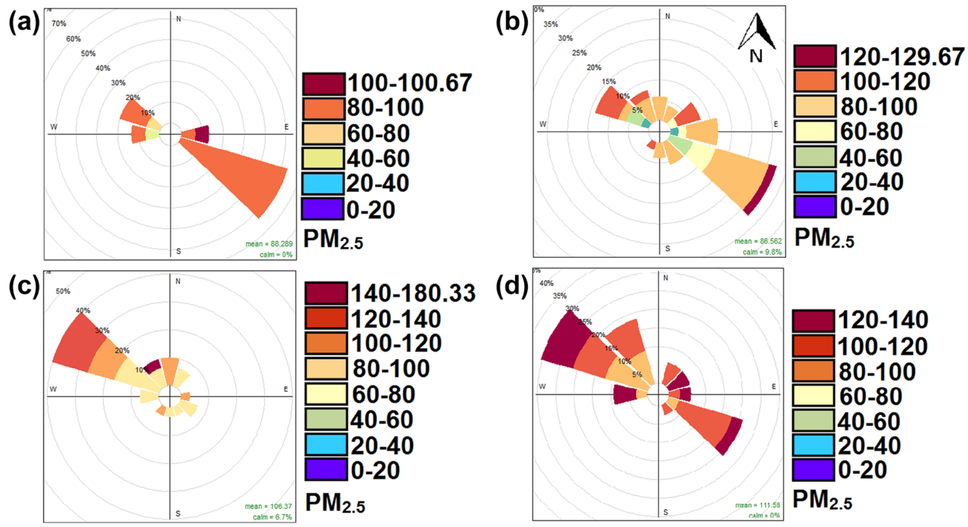

Fig. 4 Seasonal pollution roses for $PM_{2.5}$ **a** pre-monsoon, **b** monsoon, **c** post-monsoon, **d** winter

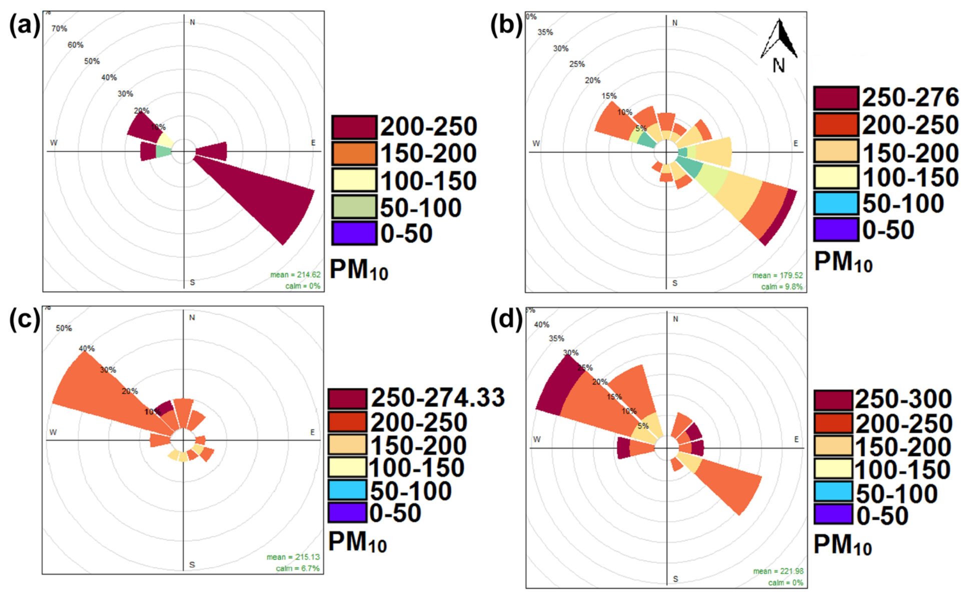

Fig. 5 Seasonal pollution roses for PM_{10} **a** pre-monsoon, **b** monsoon, **c** post-monsoon, **d** winter

During the post-monsoon season (Fig. 4c), the dominant wind direction was found to be northwesterly with a concentration ranging from 80 to 120 μg/m^3, and minor components of wind were found in the northerly direction. In the winter season (Fig. 4d), the direction with more pollution was found to be northwesterly with a concentration range of 80–120 μg/m^3. A second prevailing direction of polluted air mass was southeasterly, associated with similar concentration ranges as that of the northwesterly. Apart from these, fewer components of polluted winds were observed in the northeasterly, westerly and easterly directions with a concentration always greater than 100 μg/m^3.

By performing similar analysis for PM_{10}, results indicate that during the pre-monsoon season (Fig. 5a), winds associated with high concentrations of PM_{10} ranging from 200 to 250 μg/m^3 were found to be reaching the study site in southeasterly direction and a second dominant direction was found to be northwesterly with PM_{10} load ranging from 200–250 μg/m^3 to 100–150 μg/m^3.

In the monsoon season (Fig. 5b), the dominant wind direction was found to be southeasterly, majorly associated with a concentration > 100 μg/m^3, and a second prevailing direction was found to be northwesterly with a load majorly greater than 200 μg/m^3. Minor components of winds with a concentration load of > 100 μg/m^3 in the northeasterly and northerly direction were also noticed. In the post-monsoon season (Fig. 5c), the dominant wind direction was found to be northwesterly with a concentration of > 200 μg/m^3. During the winter season (Fig. 5d), the dominant wind direction was found to be northwesterly with a high pollution load of > 150 μg/m^3. The other prevailing direction with a load of 150–200 μg/m^3 is the southeasterly. Minor components of winds were observed in the westerly, easterly and northeasterly direction with a pollution load of > 200 μg/m^3 at the study site. Winds blowing from the marine side, i.e., the southeasterly direction, were assumed to be cleaner, but as the winds passed through the densely populated and polluted urban and industrial areas, such as Bhubaneshwar and Angul, they were contaminated by PM before reaching the study area. Components of air masses arriving at the study site from the northwest and northeast directions blow from land masses and are polluted as they carry aerosols from the highly industrialized regions of Chhattisgarh and Jharkhand. During the post-monsoon and winter, the dominant wind direction is the northwest which is responsible for regional transport of transboundary pollutants to the study site from parts of Madhya Pradesh and Chhattisgarh, associated with limestone, cement and other industries. These results are justified by CPF and CPBF techniques in the later sections.

During the study period, the seasonal variation of $PM_{2.5}$, $PM_{10}$and $PM_{2.5}/PM_{10}$ showed noticeable differences for different seasons. The seasonal mean mass concentrations of $PM_{2.5}$, PM_{10} and $PM_{2.5}/PM_{10}$ for three monitoring stations are shown in Tables 2, 3 and 4 respectively. $PM_{2.5}$ seasonal variations (Table 2) depict that the concentrations are high in the pre-monsoon season, followed by winter, post-monsoon and monsoon seasons at Sonaparbat, and the pollution levels are lower in comparison to the industrial stations, but the levels always crossed the specified threshold levels. The values at Rourkela and Rajgangpur are also very high and crossed the specified threshold levels. Seasonal variations for PM_{10} also follow a similar variation for three sites (Table 3). The high amount of $PM_{2.5}$ and PM_{10} concentrations during different seasons can be elucidated as local

Table 2 Seasonal averages of $PM_{2.5}$ at Sonaparbat, Rourkela and Rajgangpur stations

$PM_{2.5}$	Year	Pre-monsoon	Monsoon	Post-monsoon	Winter
Sonaparbat	2009	112.81 ± 25.20	86.39 ± 19.62	93.62 ± 17.22	118.46 ± 24.65
	2010	100.83 ± 22.37	96.21 ± 15.55	103.37 ± 19.92	103.45 ± 18.26
	2011	102.51 ± 18.43	89.66 ± 13.96	102.17 ± 20.99	106.39 ± 19.85
	2012	103.60 ± 19.58	89.72 ± 24.80	98.85 ± 14.37	104.48 ± 18.07
	2013	123.96 ± 40.13	77.52 ± 16.14	72.66 ± 11.29	97.31 ± 23.09
	2014	76.12 ± 12.46	67.24 ± 7.34	70.18 ± 9.39	73.75 ± 12.77
Rourkela	2009	121.02 ± 20.63	108 ± 18.29	109.11 ± 18.08	121 ± 23.7
	2010	103.87 ± 20.22	106 ± 18.95	100.59 ± 11.82	116.47 ± 19.52
	2011	114.12 ± 15.81	107.87 ± 14.93	102.43 ± 12.14	108.21 ± 16.28
	2012	99.98 ± 12.73	87.82 ± 10.92	113.74 ± 19.33	97.02 ± 14.33
	2013	104.32 ± 100.96	88.69 ± 13.80	96.35 ± 13.16	95.94 ± 15.60
	2014	88.55 ± 11.85	80.65 ± 27.22	98.92 ± 23.82	92.87 ± 9.95
Rajgangpur	2013	109.46 ± 14.56	95.50 ± 11.03	94.7 ± 10.14	99.74 ± 12.15
	2014	131.23 ± 25.23	73.14 ± 45.74	117.78 ± 48.59	127.03 ± 35.61

Table 3 Seasonal averages of PM_{10} at Sonaparbat, Rourkela and Rajgangpur stations

PM_{10}	Year	Pre-monsoon	Monsoon	Post-monsoon	Winter
Sonaparbat	2009	223.12 ± 42.40	177.98 ± 33.48	193.74 ± 28.49	240.98 ± 39.16
	2010	214.07 ± 31.89	206.43 ± 28.38	209.64 ± 36.67	220.03 ± 33.39
	2011	216.57 ± 31.84	192.36 ± 22.91	220.39 ± 40.74	226.14 ± 34.10
	2012	224.38 ± 35.11	198.55 ± 46.87	206.25 ± 23.20	220.43 ± 33.01
	2013	210.29 ± 34.30	163.43 ± 32.01	129.41 ± 12.38	192.21 ± 33.75
	2014	162.06 ± 150.67	136.03 ± 11.68	136.80 ± 12.63	150.29 ± 32.13
Rourkela	2009	208.24 ± 30.59	198.52 ± 20.17	199.9 ± 24.3	215.87 ± 30.81
	2010	199.91 ± 25.82	208.35 ± 24.73	199.44 ± 15.09	211.12 ± 28.79
	2011	230.34 ± 34.93	203.39 ± 28.26	195.21 ± 29.95	206.24 ± 28.03
	2012	205.69 ± 30.83	179.39 ± 17.63	239.88 ± 26.38	195.3 ± 29.4
	2013	198.76 ± 24.38	182.52 ± 18.59	204.54 ± 31.17	231.03 ± 191.03
	2014	222.55 ± 38.59	170.83 ± 65.37	216.92 ± 20.10	219.46 ± 15.98
Rajgangpur	2013	222.90 ± 13.86	216 ± 16.23	225.41 ± 11.92	224.51 ± 12.00
	2014	292.01 ± 67.99	149.38 ± 95.29	234.66 ± 85.89	237.91 ± 40.15

Table 4 Seasonal averages of $PM_{2.5}/PM_{10}$ at Sonaparbat, Rourkela and Rajgangpur stations

RSPM/SPM	Year	Pre-monsoon	Monsoon	Post-monsoon	Winter
Sonaparbat	2009	0.50 ± 0.07	0.48 ± 0.04	0.48 ± 0.03	0.49 ± 0.04
	2010	0.46 ± 0.05	0.46 ± 0.03	0.49 ± 0.04	0.46 ± 0.03
	2011	0.47 ± 0.04	0.46 ± 0.03	0.46 ± 0.03	0.46 ± 0.04
	2012	0.46 ± 0.05	0.76 ± 3.19	0.47 ± 0.04	0.47 ± 0.04
	2013	0.59 ± 0.18	0.48 ± 0.11	0.56 ± 0.05	0.51 ± 0.10
	2014	0.51 ± 0.09	0.49 ± 0.05	0.51 ± 0.05	0.50 ± 0.08
Rourkela	2009	0.58 ± 0.05	0.54 ± 0.06	0.54 ± 0.07	0.56 ± 0.09
	2010	0.51 ± 0.06	0.50 ± 0.04	0.53 ± 0.04	0.53 ± 0.05
	2011	0.5 ± 0.04	0.53 ± 0.03	0.52 ± 0.05	0.52 ± 0.03
	2012	0.5 ± 0.04	0.5 ± 0.04	0.47 ± 0.07	0.5 ± 0.04
	2013	0.46 ± 0.06	0.48 ± 0.04	0.47 ± 0.04	0.45 ± 0.07
	2014	0.40 ± 0.06	0.49 ± 0.10	0.45 ± 0.07	0.42 ± 0.05
Rajgangpur	2013	0.49 ± 0.07	0.44 ± 0.04	0.41 ± 0.03	0.44 ± 0.05
	2014	0.45 ± 0.04	0.50 ± 0.10	0.49 ± 0.06	0.53 ± 0.11

emissions mixed with regional and transported pollutants, along with the combined effect of weather conditions.

The maximum values of pollutants, however, differ for the three sites seasonally. For the monitoring sites, Sonaparbat and Rajgangpur, the concentrations of $PM_{2.5}$ and PM_{10} were higher in the pre-monsoon season followed by winter, post-monsoon and monsoon during the study period. At Rourkela, high loads of $PM_{2.5}$ and PM_{10} were found in winter, followed by pre-monsoon, post-monsoon, and monsoon. However, the difference between pre-monsoon and winter seasons is small at all the three sites.

The higher concentrations during the pre-monsoon season over Sonaparbat and Rajgangpur may be attributed to mineral dust transported from the southeast and northwestern regions, along with locally emitted industrial pollution. The pre-monsoon season has a unique meteorological feature of passing Nor'westers over the area, which is also believed to transport pollution along with fluxes of mass, momentum and heat over the regions (Das et al. 2015). Surface winds during Nor'westers are found to be either southeasterly or northwesterly at the stations experiencing these Nor'westers during the pre-monsoon season (Das et al. 2014), which is evident by our surface wind observations as well (not shown here). Mineral dust is one of the significant contributors to aerosol load over the region in all the seasons (Kavuri et al. 2013).

Less variation of $PM_{2.5}$ and PM_{10} during monsoon in comparison to the other seasons may be attributed to washout of the emitted pollutants by the monsoonal rainfall during the active spell, but the values are found to be always high and crossing the threshold because winds are affected by polluted urban areas as mentioned earlier in seasonal pollution roses. High concentrations of $PM_{2.5}$ and PM_{10} during post-monsoon and winter seasons are due to locally generated pollution along with transported pollution and varying meteorological conditions like temperature. The stable atmospheric conditions associated with low wind speed and pollutant accumulation over a place during the winter season increase PM concentration (Tiwari et al. 2012). As mentioned previously, the study site is continuously exposed to the polluted northwesterly wind during the winter season, which maintains a high concentrations throughout the study period. When the seasonality of $PM_{2.5}/PM_{10}$ is considered (Table 4), at both the industrial and residential sites, the ratio is found to be high in all the seasons with a value ranging from 0.4 to 0.7 indicating the dominance of fine mode particles over the inhalable coarse mode particles in all the seasons. The ratio was high in the monsoon season for Rourkela station, indicating the dominance of $PM_{2.5}$ over PM_{10} when compared to all other seasons in spite of rainout and washout of PM, which may be due to the industrial emissions during the break spells of monsoon.

Previous studies, which carried out similar work at other parts of the world (Akinlade et al. 2015), have also reported high concentrations of $PM_{2.5}$ in the monsoon, attributed to the various anthropogenic sources present within the vicinity of the study area. As the monitoring site is associated with India's biggest steel plant and other industries including cement factories, it is understandable that fine mode particles will dominate the study site. Moreover, at Sonaparbat, in the years 2013 and 2014, the ratio of $PM_{2.5}$ to PM_{10} was found to be high when compared to the industrial sites Rourkela and Rajgangpur, indicating the exposure of residents to $PM_{2.5}$ higher when compared to PM_{10}, thereby increasing the threat of respiratory and cardiovascular diseases. In addition to this to assess the air pollution levels, seasonal air quality index (AQI) was computed in the present study for both residential and industrial areas. AQI calculation was performed using the following Eq. (5) (Rao and Rao, 1989):

$$\mathrm{AQI} = \frac{1}{2}\left[\frac{\mathrm{SPM}}{C_{\mathrm{SPM}}} + \frac{\mathrm{RSPM}}{C_{\mathrm{RSPM}}}\right] \times 100 \tag{5}$$

where C_{SPM} indicates the critical value for SPM and C_{RSPM} indicates the critical value for RSPM specified by CPCB (CPCB 2009). From the AQI values (Table 5), it is clear that Rourkela and Sonaparbat are moderately polluted in all the seasons, whereas Rajgangpur air quality was found to be poor in the pre-monsoon, post-monsoon and winter seasons and moderately polluted in the monsoon season. The presence of cement factory and iron and steel industries in Rajgangpur might be responsible for poor air quality.

Table 5 Average seasonal AQI values for three stations Rourkela (2009–2014), Sonaparbat (2009–2014), Rajgangpur (2013–2014) in pre-monsoon, monsoon, post-monsoon and winter seasons (Yellow color-moderately polluted, Red Color-Poor) (http://pib.nic.in/newsite/PrintRelease.aspx?relid=110654)

Station	Pre-monsoon	Monsoon	Post-monsoon	Winter
Rourkela	**193.2542**	**175.6775**	**193.6084**	**195.7219**
Sonaparbat	**190.2204**	**159.9582**	**170.6264**	**187.5544**
Rajgangpur	**225.2386**	**161.5179**	**203.5575**	**213.191**

5.4 Seasonal CPF and CBPF Analysis

For identifying maximum probable wind sectors that are associated with enhanced $PM_{2.5}$ and PM_{10} values CPF analysis was performed. CPF analysis for $PM_{2.5}$ and PM_{10} in the pre-monsoon, monsoon, post-monsoon and winter seasons is shown in Figs. 6 and 7 at a percentile of 20. In the pre-monsoon season (Figs. 6a,7a), it can be noticed that the east, southeast, west and northwest wind sectors were found to be contributing particulate pollution with a probability of 1 to the study area. In the monsoon season (Fig. 6b,7b), north, northwest, south, southeast and southwest wind sectors were dominant for $PM_{2.5}$, whereas northwest, northeast and southeast wind sectors contributed to the PM_{10} load. Sources of PM located in the wind sectors such as north, northeast, northwest, southeast, south and southwest were responsible for the high pollution in the post-monsoon season (Figs. 6c, 7c). In the winter season (Figs. 6d, 7d), northwest, northeast and southeast wind sectors were found to be responsible in the enhancement of particulate pollution over Rourkela.

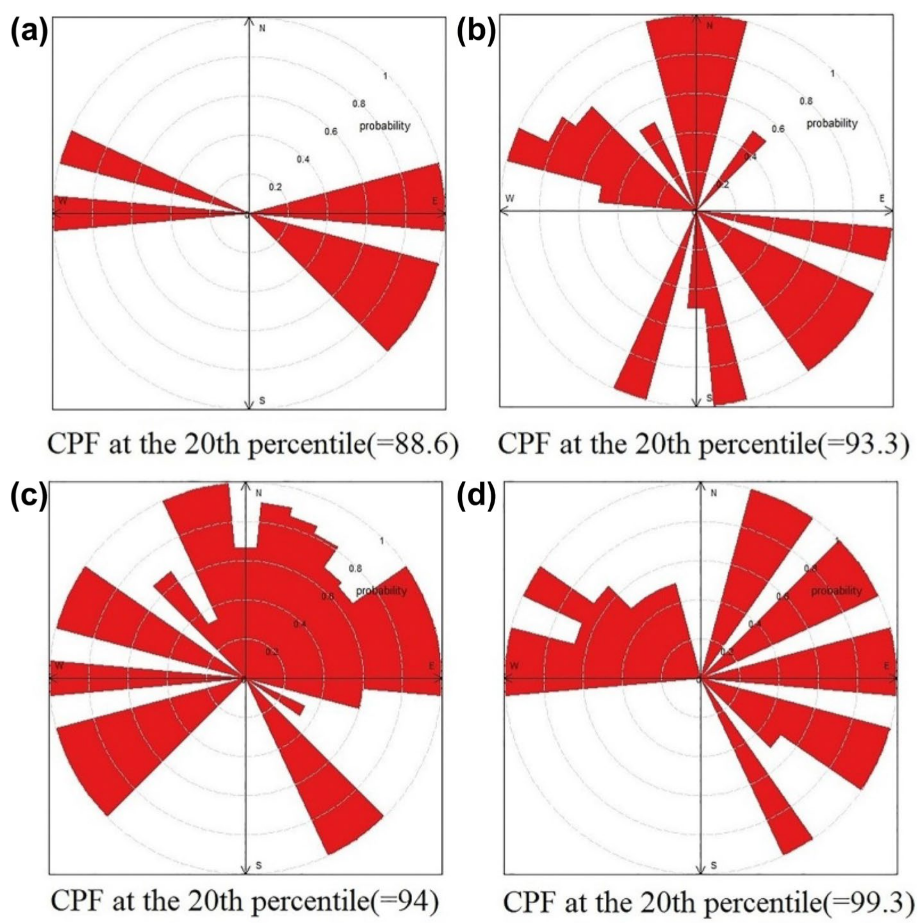

Fig. 6 Seasonal CPF plot for $PM_{2.5}$ in μg/m^3 at 20th percentile in **a** pre-monsoon, **b** monsoon, **c** post-monsoon, **d** winter seasons respectively

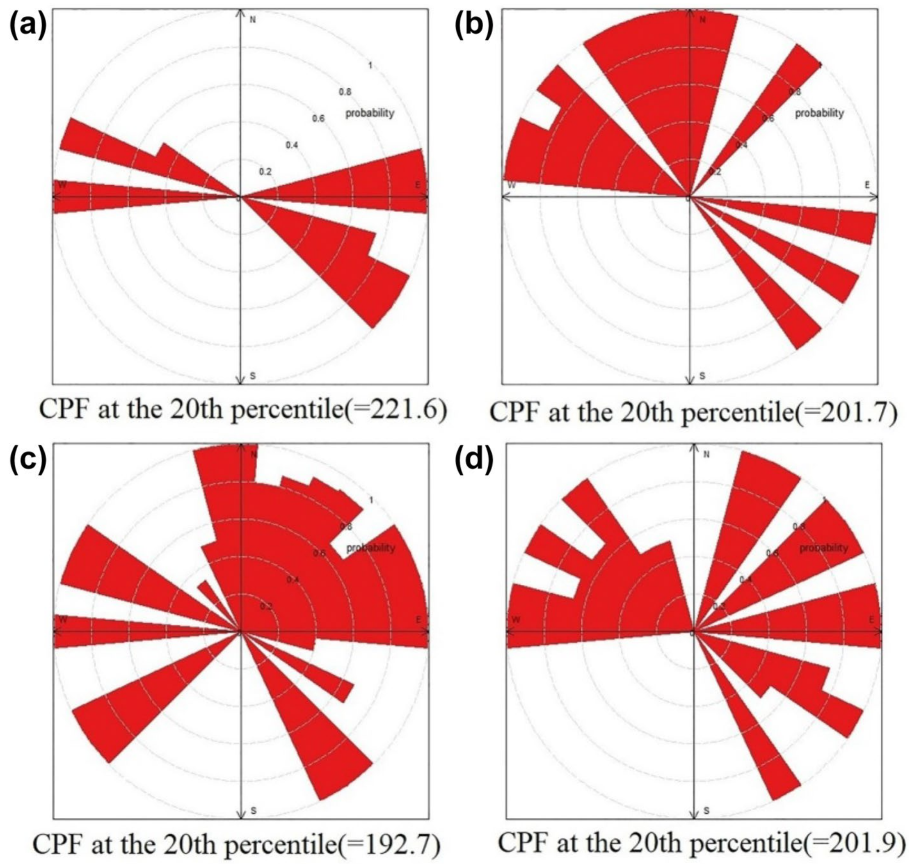

Fig. 7 Seasonal CPF plot for PM_{10} at 20th percentile in **a** pre-monsoon, **b** monsoon, **c** post-monsoon, **d** winter seasons respectively

These results justify the conclusions drawn from pollution rose plot, thereby depicting the prominent role played by wind direction in modulating the $PM_{2.5}$ and PM_{10} concentrations over the study site.

As an extension to the CPF analysis, CBPF analysis was performed using bivariate polar plots incorporating wind velocity as the third variable (Uria-Tellaetxe and Carslaw 2014; Rai et al. 2016). In the present study, we used two percentile quartiles (10–50% and 50–100%). The probability values for CBPF are shown as colored scales in Figs. 8 and 9. Figure 8 shows the CBPF analysis for $PM_{2.5}$ in the pre-monsoon, monsoon, post-monsoon and winter seasons (Fig. 8a, c, e, g with a percentile range of 10–50%, and Fig. 8b, d, f, h with a percentile range of 50–100%), respectively. In the pre-monsoon season, a dominant source with a percentile range of 10–50% (Fig. 8a) and 50–100% (Fig. 8b) located in the southeast direction resulted in high probability where wind speeds were found to be 0.5 ms^{-1}, thus indicating the highest probability of pollution due to sources near Rourkela. In the monsoon season (Fig. 8c, d), 10–50% quartile sources present in the southeast direction were found to be dominating where wind speeds did not exceed 1 ms^{-1}, and 50–100% quartile sources in the northwest and northeast directions were found to be dominating where wind speed varied from 0.5 ms^{-1} to 2 ms^{-1}. In the post-monsoon season, high probability of $PM_{2.5}$ was noticed in the southeast direction where wind speed was 2 ms^{-1} in the 10–50% quartile (Fig. 8e), and in the 50–100% quartile northwest direction was found to be a dominating source associated with wind speed 1.5 ms^{-1}. In the winter season also, for 10–50% and 50–100% quartiles (Fig. 8g, h), wind speeds were less than 1 ms^{-1} and northeast and southeast directions were the dominant sources. From CBPF analysis for $PM_{2.5}$, it can be concluded that sources present in the northwest and southeast directions dominate in all the seasons. Wind speeds did not exceed 2 ms^{-1} in all the seasons for $PM_{2.5,}$ thereby indicating the presence of sources near the study area. A similar analysis was carried out for PM_{10} to characterize sources in different seasons using the CBPF technique shown in Fig. 9 and is interpreted as in Fig. 8. The locations of sources for PM_{10} were similar to those of $PM_{2.5}$ with dominant sources existing in the northwest and southeast directions. The maximum $PM_{2.5}$ and PM_{10} concentrations were found to be occurring when wind speeds were very low (< 1.5 ms^{-1}), thereby enabling accumulation of pollutants over the study area. Urban areas located within the vicinity of the city and automobile exhaust may be responsible for the high pollution in Rourkela (Kavuri et al. 2013). As there is a scarcity of enough literature over

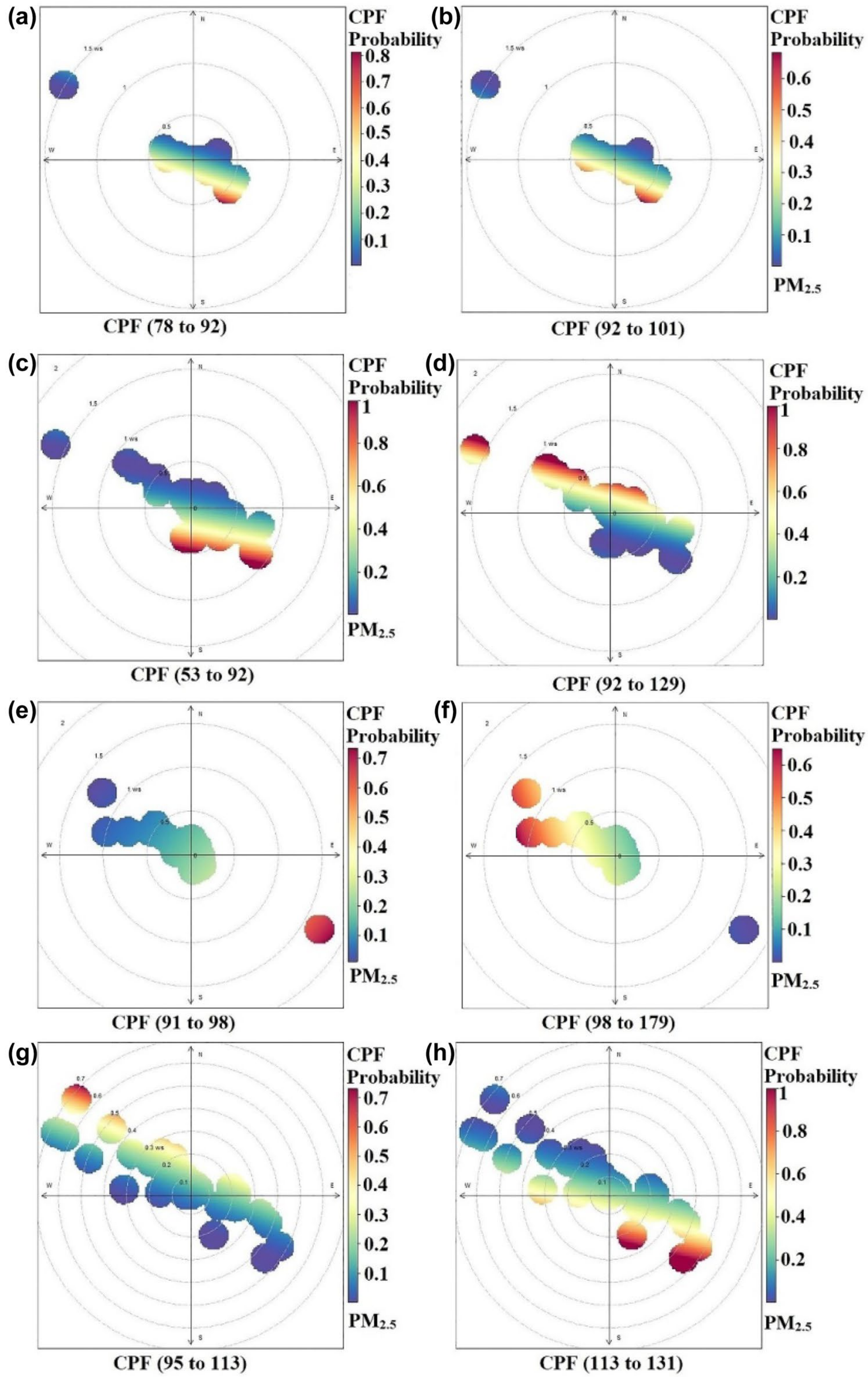

Fig. 8 Seasonal CBPF plot for $PM_{2.5}$ with two percentile quartiles 10–50% (**a**, **c**, **e**, **g**) and 50–100% (**b**, **d**, **f**, **h**) in **a**, **b** pre-monsoon. **c**, **d** Monsoon. **e**, **f** Post-monsoon. **g**, **h** Winter seasons respectively

Rourkela, evidences of particulate pollution due to cooking and heating were not found. Sources such as National Aluminium Company (NALCO), Mahanadi Coal Fields (MCL), National Thermal Power Corporation (NTPC) and Talcher Thermal Power Station (TTPS) are located in the southeast wind sector to the study area. Talcher coal area is recognized as Asia's largest coal field (https://angul.nic.in/economy). In the northwest direction, industries such as Jindal Steel and Power Limited (JSPL), ACC Rio and Tinto PVT Limited, which are mineral-based industries,

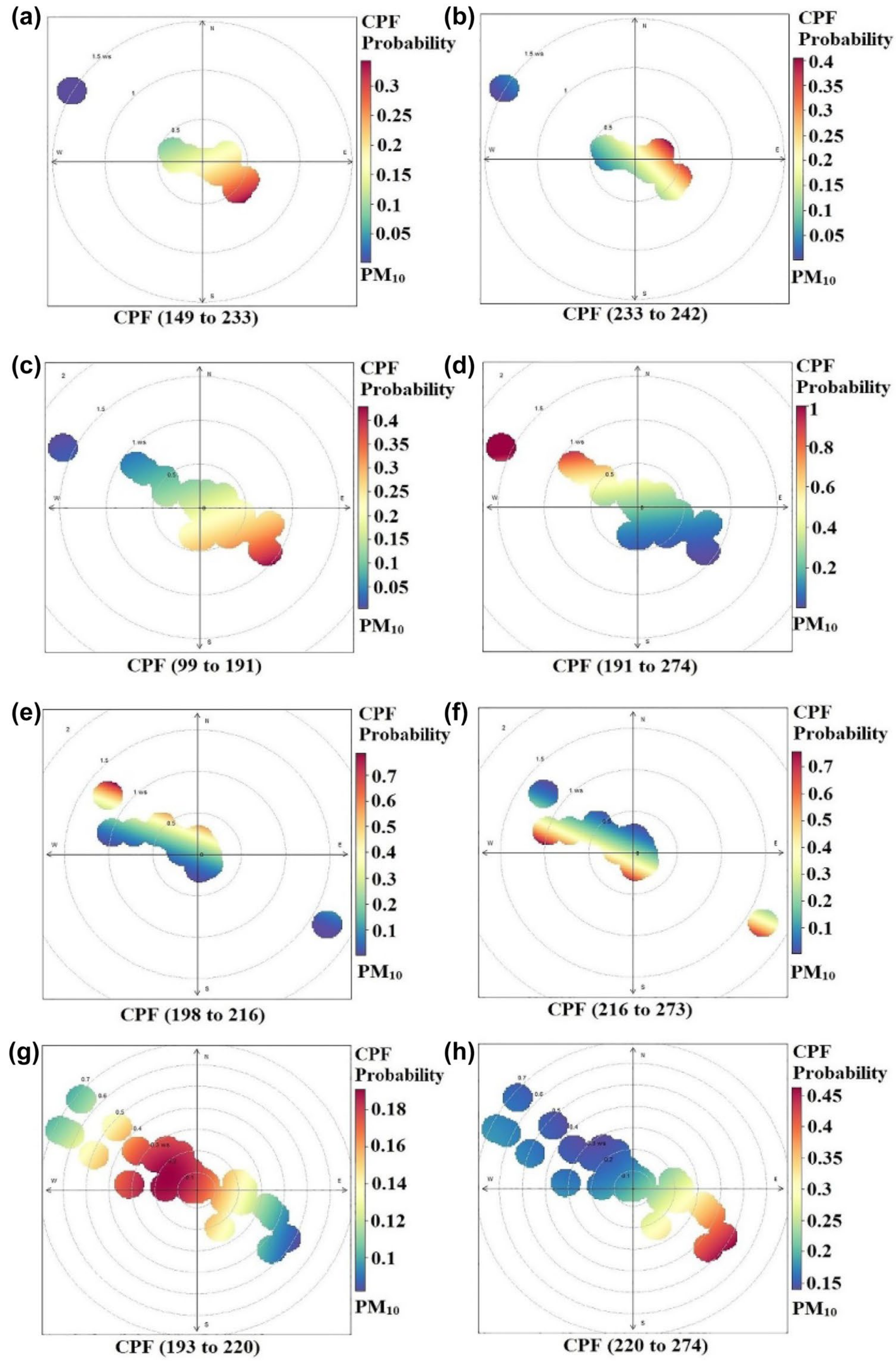

Fig. 9 Seasonal CBPF plot for PM_{10} with two percentile quartiles 10–50% (**a**, **c**, **e**, **g**) and 50–100% (**b**, **d**, **f**, **h**) in **a**, **b** pre-monsoon. **c**, **d** Monsoon. **e**, **f** Post-monsoon. **g**, **h** Winter seasons respectively

are situated (http://www.samataindia.org.in/mici/attachments/article/42/Jashpur,%20Chattisgarh.pdf).

5.5 Seasonal CWT Analysis

As mentioned earlier, CWT which helps in identifying the location and strength of the sources is used in the present study (Hsu et al. 2003; Seibert et al. 1994). In the present study, CWT is used to determine the significance of both principal and moderate sources of the measured $PM_{2.5}$ and PM_{10} concentrations at the monitoring site, Rourkela. The pollution criterion for $PM_{2.5}$ and PM_{10} was taken as 60 µg/m^3 and 100 µg/m^{3}to perform the CWT analysis. A 2 day backward (− 48 h) CWT analysis for the four seasons,

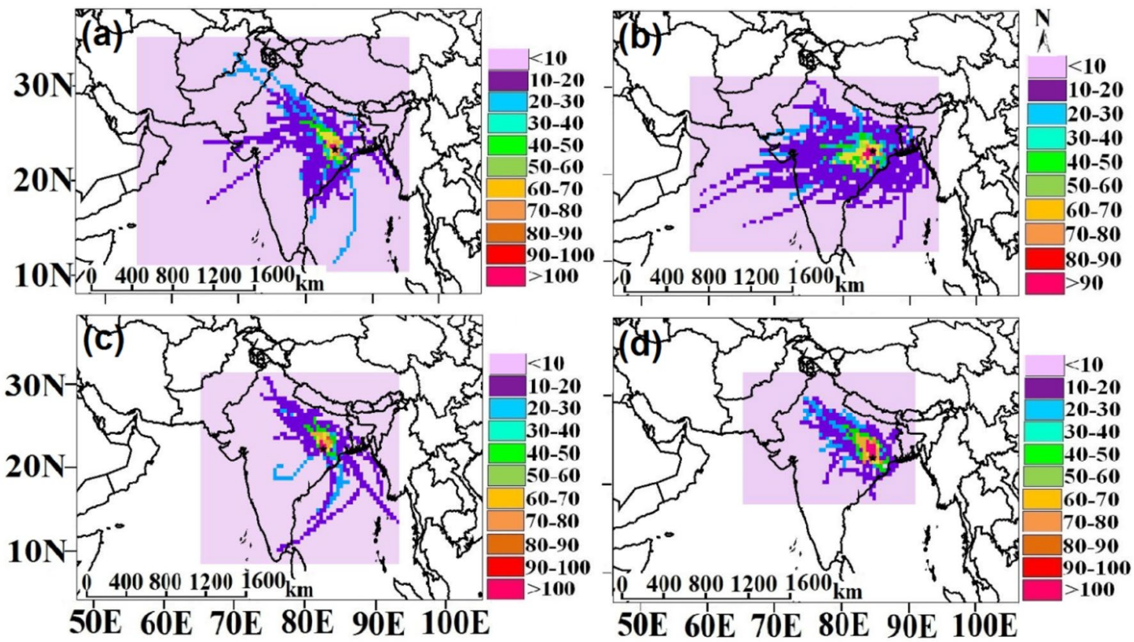

Fig. 10 Seasonal CWT analysis for − 48 h at Rourkela site for $PM_{2.5}$ in **a** pre-monsoon, **b** monsoon, **c** post-monsoon and **d** winter seasons, respectively, during the study period 2009–2014

pre-monsoon, monsoon, post-monsoon and winter, was performed to identify the source regions, and the CWT analysis for $PM_{2.5}$ and PM_{10} for the four seasons is shown in Figs. 10 and 11. The seasonal CWT analysis of $PM_{2.5}$ for the pre-monsoon season (Fig. 10a) identified Sundergarh, Sambalpur and Jharsuguda districts of Odisha, Jashpur District of Chhattisgarh and Simdega District of Jharkhand as the potential source areas. During the monsoon (Fig. 10b), Sundergarh, Jharsuguda, Sambalpur and Deogarh of Odisha are the principal source areas. Jashpur of Chhattisgarh, Sambalpur, Sundergarh and Jharsuguda of Odisha, and Simdega, Gumla and Ranchi of Jharkhand are the principal source areas in the post-monsoon season (Fig. 10c). In winter season (Fig. 10d), Sundergarh and Deogarh of Odisha, Jashpur of Chhattisgarh, and Simdega, Gumla and Lohardaga of Jharkhand are the principal source locations. Lohardaga is rich in bauxite resources (MSME Report, Lohardaga 2012).

Seasonal CWT analysis for PM_{10} in the pre-monsoon season (Fig. 11a) identified Sundergarh and Sambalpur of Odisha and Jashpur of Chhattisgarh as the principal source areas. During monsoon (Fig. 11b), Singrauli, Balaghat and Sidhi of Madhya Pradesh, Gondia, Bhandara, Nagpur and Chandrapur of Maharashtra, North Chhattisgarh, Simdega, West Singhbum, Khunti, Ranchi, Gumla and Lohardaga of Jharkhand, Sundergarh, Sambalpur, Jharsuguda, Deogarh, Kendujhargarh, Barjpada, Bargarh, Sonapur, Balangir, Angul, Mohpara and Bhawanipatna of Odisha are the principal source areas. Singrauli has a large-scale cement industry which lies in the northwest direction to the receptor site. Balaghat is in the southwest direction to the receptor site and has various minerals such as copper ore, manganese ore and stone and its associated industries. Sidhi lies in the northwest direction and is associated with limestone and bauxite mineral resources and a large-scale cement industry (MSME Report, Singrauli 2016, MSME Report, Balaghat 2012 and MSME Report, Sidhi 2012). Gondia, Bhandara, Nagpur and Chandrapur lie in the southwest direction to Rourkela. Gondia has minerals such as iron ore and quartz. Bhandara has manganese ore, quartz and kyanite (MSME Report, Gondia 2012). Nagpur has coal mines, manganese ore, dolomite, limestone, iron ore, clay, copper ore and chromites (MSME Report, Nagpur 2012). Chandrapur has coal mines, iron and limestone mineral resources (MSME Report, Chandrapur 2012). Chandrapur is associated with India's biggest thermal power station based on coal. Apart from the coal-based thermal power plant, it also has cement industries, which are responsible for transporting pollutants from source locations to the receptor site, Rourkela. During the post-monsoon season (Fig. 11c), Sundergarh, Sambalpur and Jharsuguda of Odisha and Simdega, Khunti and Gumla of Jharkhand are the principal source regions. Sources identified in the CBPF analysis have also been identified in CWT analysis along with the other moderate sources situated in different states such as Madhya Pradesh and Maharashtra, which explains that the state of pollution over Rourkela is not only because of the strong emission sources present within the vicinity of the study area but also due to transboundary particulate pollution. Various mineral-based industries

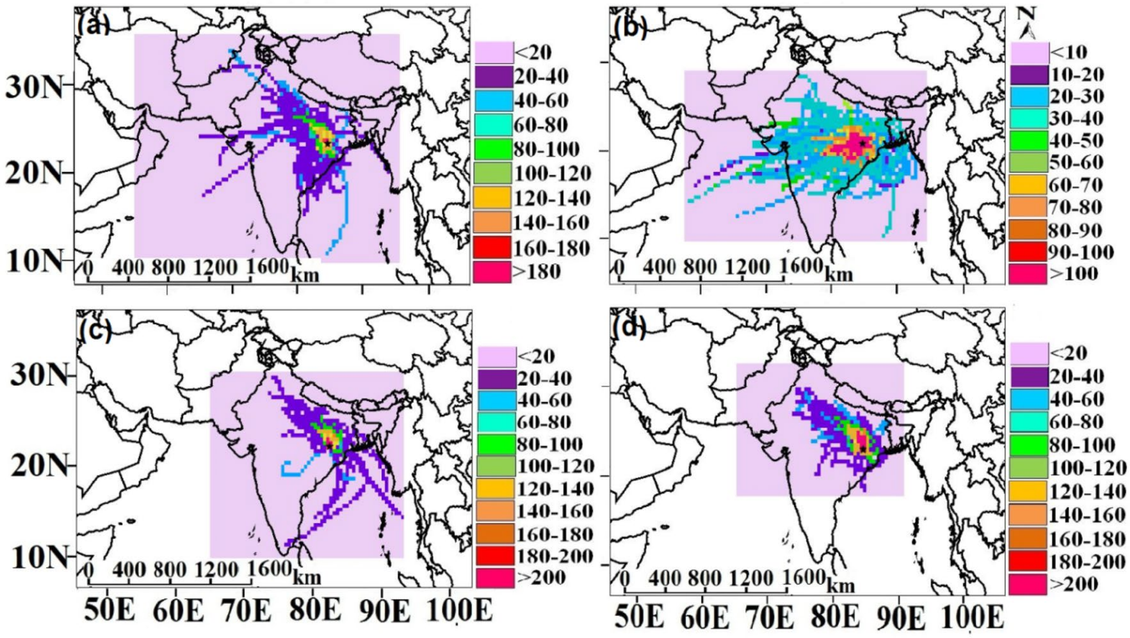

Fig. 11 Seasonal CWT analysis for − 48 h at Rourkela site for PM_{10} in **a** pre-monsoon, **b** monsoon, **c** post-monsoon and **d** Winter seasons, respectively, during the study period 2009–2014

present within a spatial extent of 200 km to the study area were found to contribute to high pollution during the study period in all the seasons. Steel and mineral-based industries (e.g., Bokaro Steel Plant, sponge iron plant, chemical and fertilizer industries, graphite, quartzite industries, calcium carbide and lime related industries) are situated in the state of Jharkhand and located in the northeast direction to the study area (https://jharkhandindustry.gov.in/mineral-based-industry). In the southwesterly direction, industries in Jharsuguda, Sambalpur and Raigarh are situated within a spatial extent of 100–200 km from the study area. The world's second largest and India's biggest sponge iron plant is situated in Raigarh, which is at a spatial distance of 162 km from the study area in the southwesterly direction. In the northeasterly direction, steel and many other mineral-based industries are situated in the Chhattisgarh districts of Jashpuranagar. In the west of Rourkela, Korba District which is referred to as the power capital of India, where a super thermal power plant is situated at a spatial distance of ~ 200 km from the study area. These industries were found to be modulating the PM concentrations in all the seasons and are identified as the principal sources by CBPF and CWT analysis.

5.6 Forward Trajectory Analysis

As forward trajectories help in understanding the dispersion of pollutants from source areas to the receptor sites, 2 days (i.e., 48 h) forward trajectory analysis was employed in the present study for the period 2012–2014 (run every 6 h using

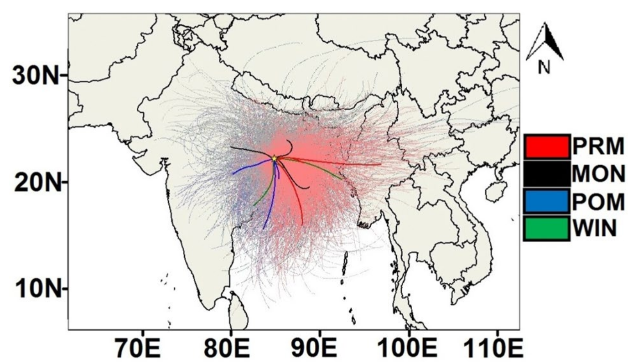

Fig. 12 Two days forward trajectories for pre-monsoon (red), monsoon (black), post-monsoon (blue) and winter (green) for the period of 2012–2014. A yellow star marks the location of the study area

GDAS 1° data by HYSPLIT4 model), as shown in Fig. 12 for different seasons. From the figure, it can be observed that the polluted air masses are more likely to contribute to the pollution of the Indo-Gangetic plain, parts of central India and eastern states of India in different seasons. Zooming into local scales, during the pre-monsoon season, the trajectories pass through the densely populated regions of Odisha (Angul and Bhubaneshwar) toward the Bay of Bengal in the southeasterly direction and Madhya Pradesh in the northwest direction and Jharkhand in the northeast direction.

In the monsoon season, the air masses were found to be traversing through Madhya Pradesh in the northwest, Jharkhand in the northeast, and Angul and Bhubaneshwar in the southeast direction toward the Bay of Bengal. In the post-monsoon season, Chhattisgarh and the eastern part of Maharashtra in the southwest and southeastern part of Odisha were found to experience the air masses that originated at the study site. During the winter season, air masses were found to sink at the southeastern part of Odisha, eastern coastal Andhra Pradesh and western parts of West Bengal. The analysis indicates that pollutants are dispersed mostly in the southeastern parts of Odisha, which are densely populated regions, in all the seasons. Thus, the pollution generated and accumulated over the region adds to the high loads of anthropogenic pollution over a region of a densely populated area in the State of Odisha, as well as other nearby states.

6 Conclusion

Identification of potential source regions (local and non-local) of $PM_{2.5}$ and PM_{10} over the industrial area of Rourkela was investigated in the present study using CPF, CBPF and CWT. Observations indicate that the study region is humid (relative humidity > 60%) throughout the year except for a few days of the pre-monsoon season when high temperatures exist and thunderstorms occur. The findings can be summarized as follows:

- From the annual average ratio of $PM_{2.5}/PM_{10}$, it is clear that the residential site, Sonaparbat, is more loaded with fine mode particles when compared to the industrial sites. When seasonality of ratio $PM_{2.5}/PM_{10}$ is considered, the ratio was found to be high at Sonaparbat in 2013 and 2014 and comparable to the ratios of Rourkela and Rajgangpur in the rest of the years indicating the severity of $PM_{2.5}$ load over the residential site.
- From seasonal pollution roses, CPF and CBPF plots, winds in the southeasterly (marine in nature) direction and the northwesterly and northeasterly (continental in nature) directions were found to be polluted as they are profoundly influenced by the highly populated, polluted urban and industrial areas by the time they arrive at the study site. Iron and steel industries, coal-based thermal power plants and mineral-based industries present within the vicinity 200 km from the study area are identified as the sources.
- CWT analysis identified regions of Odisha, Jharkhand and Chhattisgarh states, which are rich in mineral resources, as well as various large-, medium- and small-scale industries as primary sources for transported $PM_{2.5}$ and PM_{10} over the study region at regional scales. Along with the industrial air pollution vehicular exhaust is also responsible for high particulate pollution over the study area.
- The forward trajectory analysis shows that Indo-Gangetic plain, central India and eastern India (Odisha, Jharkhand) are the regions that receive a load of highly polluted air in the study area. The results show that the polluted air masses not only impact nearby cities, but also the cities of neighboring states in a seasonal pattern.

The results are noteworthy for policy makers for assessing the state of pollutants and improving implementations for a cleaner environment over the region of study. The results are also useful for researchers from other regions of the world for a better understanding of change in pollution concentration of industrialized areas by keeping the maximum limit of production with improved fuel inputs, and plant sampling to prevent pollution beyond the threshold limits over any region.

Acknowledgements Ms. Priyanjali Gogikar would like to acknowledge the National Institute of Technology Rourkela for providing fellowship for conducting research. The authors acknowledge the Indian Space Research Organization (ISRO) for providing the wind data through MOSDAC, NCEP/NCAR for supplying GDAS 1° data and NOAA for the HYPLIT4 model. The authors also want to acknowledge the pollution control board team members, who showed their dedication in collecting these observations.

Compliance with Ethical Standards

Conflict of interest On behalf of all the authors, the corresponding author states that there is no conflict of interest.

References

Akinlade GO, Olaniyi HB, Olise FS, Owoade OK, Almeida SM, Almeida-Silva M, Hopke PK (2015) Spatial and temporal variations of the particulate size distribution and chemical composition over Ibadan, Nigeria. Environ Monit Assess 187(8):544

Begum BA, Kim E, Jeong CH, Lee DH, Hopke PK (2005) Evaluation of the potential source contribution function using the 2002 Quebec forest fire episode. Atmos Environ 39:3719–3724

Briggs NL, Long CM (2016) Critical review of black carbon and elemental carbon source apportionment in Europe and the United States. Atmos Environ 144:409–427

Census Report (2011) The Registrar General & Census Commissioner, India (http://www.censusindia.gov.in/2011census/population_enumeration.html)

Cheng I, Zhang L, Balanchard P, Dalzei J, Tordan R (2013) Concentration weighted trajectory approach to identifying potential sources of speciated atmospheric mercury at an urban coastal site in Nova Scotia, Canada. Amos Chem Phys 13:6031–6048

Cheng I, Zhang L, Xu X (2016) Impact of measurement uncertainties on receptor modeling of speciated atmospheric mercury. Sci Rep 6(20676):1–11

CPCB Report (2009) National Ambient Air Quality Standards (NAAQS), Gazette Notifcation, New Delhi

CPCB Report (2015) National Air Quality Index. Series: CUPS/82/2014-15, pp 58
Das S, Mohanty UC, Tyagi A, Sikka DR, Joseph PV, Rathore LS, Habib A, Baidya S, Sonam K, Sarkar A (2014) The SAARC STORM - a coordinated field experiment on severe thunderstorm observations and regional modeling over the south Asian region. Bull Am Meteorol Soc 95(4):603–617
Das S, Sarkar A, Das MK, Rahman MM, Islam MN (2015) Composite characteristics of Nor'westers based on observations and simulations. Atmos Res 158:158–178
Dimitriou K (2015) The dependence of PM size distribution from meteorology and local-regional contributions, in Valencia (Spain)—a CWT approach. Aerosol Air Qual Res 15:1979–1989
Dominici F, Greenstone M, Sunstein CR (2014) Particulate matter matters. Science 344:257–259
Draxler RR (1999) HYSPLIT4 user's guide. NOAA Tech. Memo. ERL ARL-230, NOAA Air Resources Laboratory, Silver Spring, MD
Draxler RR, Hess GD (1997) Description of the HYSPLIT_4 modelling system. NOAA Tech. Memo. ERL ARL-224, NOAA Air Resources Laboratory, Silver Spring, MD, p 24
Draxler RR, Hess GD (1998) An overview of the HYSPLIT_4 modeling system for trajectories, dispersion, and deposition. Aust Meteor Mag 47:295–308
Garg A, Shukla PR, Bhattacharya S, Dadhwal VK (2001) Subregion (district) and sector level SO_2 and NOx emissions for India: assessment of inventories and mitigation flexibility. Atmos Environ 35:703–713
Gogikar P, Tyagi B (2016) Assessment of particulate matter variation during 2011–2015 over a tropical station Agra, India. Atmo Environ 147:11–21
Grigoras G, Cuculeanu V, Ene G, Mocioaca G, Deneanu A (2012) Air pollution dispersion modeling in a polluted industrial area of complex terrain from Romania. Rom Rep Phys 64(1):173–186
Guttikunda SK, Gurjar BR (2012) Role of meteorology in seasonality of air pollution in megacity Delhi, India. Environ Monit Assess 184:3199–3211
Health Effects Institute (HEI) (2018) State of global air 2018. Special Report. Health Effects Institute, Boston
Hsu YK, Holsen TM, Hopke PK (2003) Comparison of hybrid receptor models to locate PCB sources in Chicago. Atmos Environ 37:545–562
Jayamurugan R, Kumaravel B, Palanivelraja S, Chockalingam MP (2013) Influence of temperature, relative humidity and seasonal variability on ambient air quality in a coastal urban area. Int J Atmos Sci. https://doi.org/10.1155/2013/264046
Karagulian F, Belis CA, Dora CFC, Prüss-Ustün AM, Bonjour S, Adair-Rohani H, Amann M (2015) Contributions to cities' ambient particulate matter (PM): a systematic review of local source contributions at global level. Atmos Environ 120:475–483
Karar K, Gupta AK, Kumar A (2006) Characterization and identification of the sources of chromium, zinc, lead, cadmium, nickel, manganese and iron in PM_{10} particulates at the two sites of Kolkata, India. Environ Monit Assess 120:347–360
Kavuri NC, Paul KK and Roy N (2013) Regression modeling of gaseous air pollutants and meteorological parameters in a steel city, Rourkela. India Res J Recent Sci 285–289
Kotchenruther RA (2016) Source apportionment of $PM_{2.5}$ at multiple Northwest US sites: assessing regional winter wood smoke impacts from residential wood combustion. Atmos Environ 142:210–219
Lakshmi DD, Murty PLN, Bhaskaran PK, Sahoo B, Kumar TS, Shenoi SSC, Srikanth AS (2017) Performance of WRF-ARW winds on computed storm surge using hydrodynamic model for Phailin and Hudhud cyclones. Ocean Eng 131:135–148
Li Z, Hopke PK, Husain L, Qureshi S, Dutkiewicz VA, Schwab JJ, Demerjian KL (2004) Sources of fine particle composition in New York city. Atmos Environ 38(38):6521–6529
Li Y, Chang M, Ding S, Wang S, Ni D, Hu H (2017) Monitoring and source apportionment of trace elements in PM 2.5: implications for local air quality management. J Environ Manage 196:16–25
Liu Q, Baumgartner J, Zhang Y, Schauer JJ (2016) Source apportionment of Beijing air pollution during a severe winter haze event and associated pro-inflammatory responses in lung epithelial cells. Atmos Environ 126:28–35
Masiol M, Hopke PK, Felton HD, Frank BP, Rattigan OV, Wurth MJ, LaDuke GH (2017) Source apportionment of $PM_{2.5}$ chemically speciated mass and particle number concentrations in New York City. Atmos Environ 148:215–229
MSME Report Balaghat (2012) Micro, Small and Medium enterprises development institute Udyog Vihar, Ministry of MSME, Government of India, p 12
MSME report Chandrapur (2012) Micro, Small and Medium enterprises development institute Nagpur, Ministry of MSME, Government of India, p 25
MSME Report Gondia (2012) Micro, Small and Medium enterprises development institute Nagpur, Ministry of MSME, Government of India, p 23
MSME Report Lohardaga (2012) Micro, Small and Medium enterprises development institute Ranchi, Ministry of MSME, Government of India, p 13
MSME Report Nagpur (2012) Micro, Small and Medium enterprises development institute Nagpur, Ministry of MSME, Government of India, p 18
MSME Report Sidhi (2012) Micro, Small and Medium enterprises development institute Udyog Vihar, Ministry of MSME, Government of India, p 16
MSME Report Singrauli (2016) Micro, Small and Medium enterprises development institute Indore, Ministry of MSME, Government of India, p 13
Nel A (2005) Air pollution-related illness: effects of particles. Science 308:804–806
Pekney NJ, Davidson CI, Robinson A, Zhou L, Hopke PK, Eatough D, Rogge WF (2006) Major source categories for $PM_{2.5}$ in Pittsburgh using PMF and UNMIX. Aerosol Sci Technol 40:910–924
Querol X, Alastuey A, Ruiz CR, Artiñano B, Hansson HC, Harrison RM, Straehl P (2004) Speciation and origin of PM_{10} and $PM_{2.5}$ in selected European cities. Atmos Environ 38(38):6547–6555
Rai P, Chakraborty A, Mandariya AK, Gupta T (2016) Composition and source apportionment of PM_1 at urban site Kanpur in India using PMF coupled with CBPF. Atmos Res 178(179):506–520
Rao MN, Rao HVN (1989) Air pollution indices: air pollution. Tata McGraw-Hill Publishing Ltd, New Delhi, pp 271–272
Ray K, Bandopadhyay BK, Sen B, Sharma P (2014) Thunderstorms 2014- A Report SAARC storm project 2014. IMD Report Number: ESSO/IMD/SMRC STORM Project-2014/01(2014)/03, India Meteorological Department, Ministry of Earth Sciences, Government of India
SAIL Annual Report (2016) Steel Authority of India Limited Annual report 2015-2016, p 164. https://www.sail.co.in/financial-list/103
Saraf AK, Bora AK, Das J, Rawat V, Sharma K, Jain SK (2010) Winter fog over the Indo-Gangetic plains mapping and modeling using remote sensing and GIS. Nat Hazards 58(1):199–220
Sarasamma JD, Narayanan BK (2014) Air quality assessment in the surroundings of KMML industrial area, Chavara in Kerala, South India. Aerosol Air Qual Res 14(6):1769–1778
Seibert P, Kromp-Kolb H, Baltensperger U, Jost DT, Schwikowski M (1994) Trajectory analysis of high-alpine air pollution data. In: Gryning SE, Millán MM (eds) Air pollution modeling and

its application X. NATO. Challenges of modern society, vol 18. Springer, Boston, MA
Stein AF, Draxler RR, Rolph GD, Stunder BJB, Cohen MD, Ngan F (2015) NOAA's HYSPLIT atmospheric transport and dispersion modeling system. Bull Amer Meteor Soc 96:2059–2077
Su L, Yuan Z, Fung JCH, Lau AKH (2015) A comparison of HYSPLIT backward trajectories generated from two GDAS datasets. Sci Total Environ 506(507):537
Sugimoto N, Shimizu A, Matsui I, Nishikawa M (2016) A method for estimating the fraction of mineral dust in particulate matter using PM 2.5-to-PM 10 ratios. Particuology 28:114–120
Tiwari S, Srivastava AK, Bisht DS, Safai PD, Parmita P (2012) Assessment of carbonaceous aerosol over Delhi in the Indo-Gangetic Basin: characterization, sources, and temporal variability. Nat Hazards 65:1745–1764
Tiwari S, Dumka UC, Gautam AS, Kaskaoutis DG, Srivastava AK, Bisht DS, Chakrabarty RK, Sumlin BJ, Solmon F (2017) Assessment of over Guwahati in Brahmaputra River Valley: temporal evolution, source apportionment and meteorological dependence. Atmos Pol Res 8(1):13–28
Uria-Tellaetxe I, Carslaw DC (2014) Conditional bivariate probability function for source identification. Environ Model Soft 9:1–9
U.S. EPA (2004) Air quality criteria for particulate matter (Final Report, Oct 2004). U.S. Environmental Protection Agency, Washington, DC, EPA 600/P-99/002aF-bF, 2004
Wang J, Martin ST (2007) Satellite characterization of urban aerosols: importance of including hygroscopicity and mixing state in the retrieval algorithms. J Geophys Res Atmos 112:1–18

Ms. Priyanjali Gogikar is currently pursuing her Doctoral Degree at National Institute of Technology Rourkela. She has completed her Masters (M.Tech.) in Spatial Information Technology. Her area of research is air quality assessment.

Dr. Bhishma Tyagi is working as an Assistant Professor at the Department of Earth and Atmospheric Sciences, National Institute of Technology Rourkela, Odisha, India. His area of research includes atmospheric boundary layer dynamics, air quality studies and atmospheric modeling.

Ms. Rashmi Rekha Padhan is currently working as an Assistant Environmental Scientist at Odisha State Pollution Control Board, India. She is an expert in monitoring air and water quality and is associated with pollution assessment over the state.

Dr. Mukesh Mahaling is Regional Officer, and Environmental Scientist in Odisha Pollution Control Board, India. Dr. Mahaling completed his Ph.D. from Utkal University, Bhubaneswar, India, and has 20 years of experience in dealing with air and water quality pollution measurement and analysis. Dr. Mahaling has attended many national and international seminar/workshop/training programmes as visiting and resource person in India.